the harmonics are now undistinguishable from the quantisation noise. For this case, SINAD = 62.2 dB (ENOB = 10 bit).

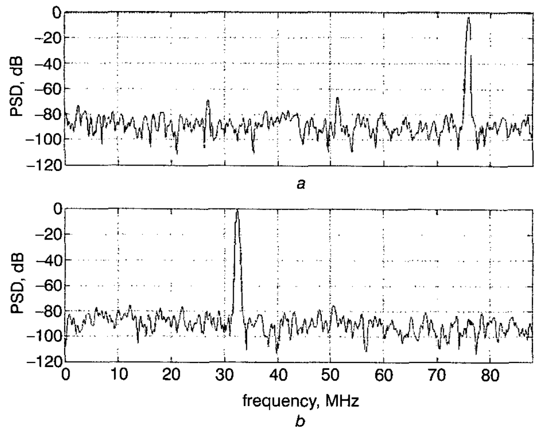

Fig. 3 *PSD of DAC output*
a f_{in} = 75.79 MHz
b f_{in} = 32.48 MHz

 31 July 2002

Electronics Letters Online No: 20020830
DOI: 10.1049/el:20020830

G. Manganaro (*Engim Inc., 40 Nagog Park, Acton, MA 01720, USA*)
E-mail: gabriele.manganaro@ieee.org

References

1 RAZAVI, B.: 'Principles of data conversion system design' (IEEE Press, 1995)
2 MALOBERTI, F., *et al.*: 'Design considerations on low-voltage low-power data converters', *IEEE Trans. Circuits Syst. I*, 1995, **42**, (11), pp. 853–863
3 WANG, F.-J., TEMES, G.C., and LAW, S.: 'A quasi-passive CMOS pipeline D/A converter', *IEEE Int. J. Solid-State Circuits*, 1989, **24**, (6),
4 KHANOYAN, K., *et al.*: 'A 10 b, 400 MS/s glitch-free CMOS D/A converter'. Proc. IEEE 1999 Symp. on VLSI Circuits, 1999, pp. 73–76, Kyoto, Japan
5 GREGORIAN, R., and TEMES, G.C.: 'Analog MOS integrated circuits for signal processing' (Wiley, 1986)

Single-chip inverter for active filters

M.K. Darwish

Generally inverter-based active filters, which employ pulse-width-modulated (PWM) techniques, use microprocessors for overall control and discrete logic for the generation of switching patterns. Because of the complexity of control required, discrete logic circuits tend to have a very high component count, making system design inflexible, expensive and less reliable than integrated circuit implementation. The work reported here presents a novel design of a single-chip controlled PWM inverter-based active filter, which addresses these issues.

Introduction: The majority of power electronics active filters, which control current harmonics, employ pulse-width-modulation (PWM) inverter circuits [1]. Since a designer has to choose the appropriate switching pattern for a given application from a wide variety of modes, every design has to be either customised or use a large number of discrete logic components to achieve flexibility. A VLSI chip (MA838) which could be suitable for such application has recently become available [2]. This Letter demonstrates that design of inverters using such a custom chip can achieve the flexibility demanded in active filter applications.

Main features: An asynchronous method of generation of PWM pattern is used with uniform or 'double-edged' regular sampling of the waveform stored in the internal ROM as shown in Fig. 1. The triangle carrier wave frequency is selectable up to 24 kHz (with maximum clock frequency of 12.5 MHz), enabling ultrasonic operation for noise-critical applications. Power frequency ranges of up to 4 kHz are possible, with the actual output frequency resolved to 12-bit accuracy within the chosen range in order to give, for example, precise motor speed control and smooth frequency changing. In theory the states of the pairs of switches of the bridge inverter are always complementary. However, owing to the finite and non-equal turn-on and turn-off times of power devices, it is desirable when changing the state of the output pair to provide a short delay time (underlap), during which both outputs are off in order to avoid a short circuit through the switching elements. Also, a pure PWM sequence produces pulses which can vary in width between 0 and 100% of the duty cycle. Therefore, in theory, pulse widths can be very narrow. In practice this causes problems in the power switches owing to charge effects and therefore a minimum pulse width is required. With the MA838 the PWM output pulses can be 'tailored' to the inverter characteristics by defining the minimum allowable pulse width (the chip will delete all shorter pulses from the 'pure' PWM pulse train) and the pulse delay (underlap) time without the need for external circuitry. The above requirements are shown in Fig. 2. These features give cost advantages on both component savings and in allowing the same PWM circuitry to be used for control of a number of different drive circuits by simply changing the microprocessor software. Power frequency amplitude control is also provided, simplifying in this way the closed-loop control circuit for controlling current harmonics.

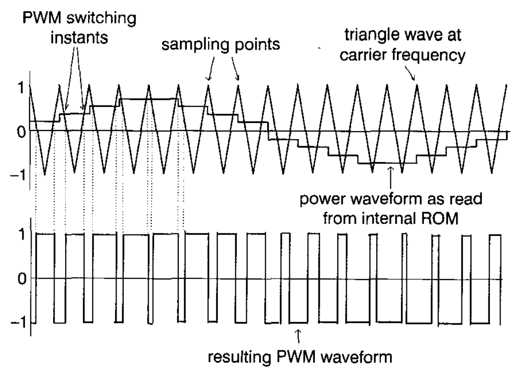

Fig. 1 *Asynchronous PWM generation by MA838-2*

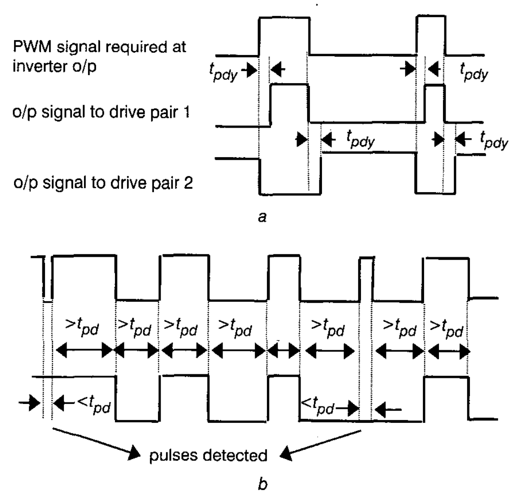

Fig. 2 *PWM pulses 'tailored' to the inverter characteristics*
a Impact of pulse delay (t_{pdy})
b Impact of pulse deletion (t_{pd})

Application: The MA838 controlled inverter was implemented and tested as part of an active filter. To control the current harmonics the MA838-2 was selected to provide a predetermined 'anti-phase' current harmonics. The MA838-2 has two 24-bit registers for loading the required parameters. The data to be loaded into either of the 24-bit register is first written to three 8-bit temporary registers before being transferred to the desired 24-bit register. Owing to this feature the chip can be easily interfaced with standard microprocessors such as 8085, 8088 (Intel) and 6800, 6805 (Motorola). The MA838-2 was interfaced with the 8085 microprocessor as shown in Fig. 3. The carrier frequency was set to 11.718 kHz with a clock of 12 MHz. The maximum carrier frequency possible (23.437 kHz), was not selected because at this frequency the MA838 was unstable. The pulse delay and the pulse deletion time were set to 0.17 μs due to the high carrier frequency. The MA838 was set to control the inverter-based active filter for three different outputs: 50 Hz–240 V, 60 Hz–110 V and 400 Hz–50 V. These modes were obtained using selection switches without any hardware modifications at all. Fig. 4 shows the spectrum of the inverter voltage and the resulting 240 V, 50 Hz filtered output with 0.9 modulation index(m). The transformer step-up ratio is 1:8 and the output filter in Fig. 3 is a combination of the transformer's magnetic leakage inductance and an 8 μF capacitor.

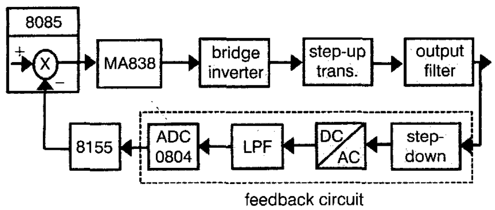

Fig. 3 *Closed-loop control system implementing MA838-2*

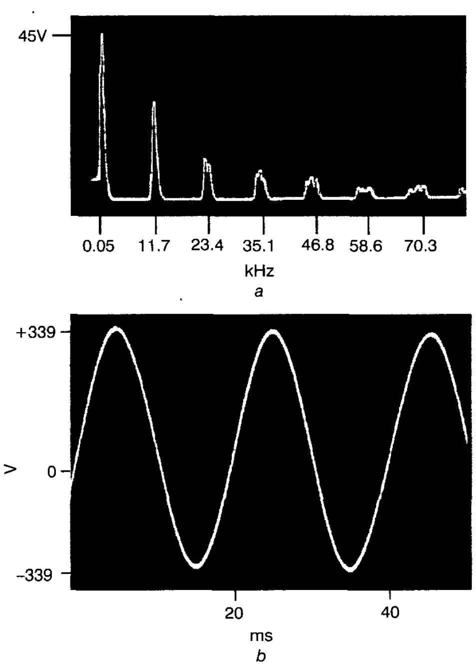

Fig. 4 *Inverter output with 50 V DC supply $m = 0.9$, $f_{carrier} = 11.718$ kHz*

a Measured inverter spectrum
b Filtered inverter output voltage

Conclusion: Commercially available chips such as the MA838 in conjunction with a microprocessor can provide the ability to implement different modes of PWM control for modern active filters requiring frequency and output voltage selection without any hardware modifications or adjustments. The component count for typical applications can be reduced considerably, saving time, reducing complexity and increasing reliability. The ability to set high carrier frequency has also simplified the design of the output lowpass filter.

 5 March 2002
Electronics Letters Online No: 20020814
DOI: 10.1049/el:20020814

M.K. Darwish (*Brunel University, Department of Electronic and Computer Engineering, Uxbridge, Middlesex UB8 3PH, United Kingdom*)

References

1 EL-HABROUK, M., DARWISH, M.K., and MEHTA, P.: 'Active power filters – a review', *IEE Proc., Electr. Power Appl.*, 2000, **147**, (5), pp. 403-413
2 GEC Plessey Semiconductor: 'Consumer IC Handbook', September 1999, pp. 6-3–6-27(Publication No. 3120)

Investigation of properties of electrical-small spherical ceramic antennas

J.R. James and J.C. Vardaxoglou

The fundamental properties of electrically small material loaded antennas are investigated by analysis of a spherical model. Data for antenna Q, resonance and efficiency demonstrate the new concept of compatible boundary conditions and its implication for practical design, particularly for mobile phones.

Introduction: There has been a recent upsurge of widespread interest in creating innovative electrically-small antennas for mobile telephone handsets. Normal mode helical antennas (NMHA) and planar inverted-F antennas (PIFA), etc., have received much attention but ceramic coated antennas [1–4] now appear to offer significant advantages particularly for integration within the handset case. This has raised many questions about the choice of the material coating with regard to: minimising absorption in the hand and head, as measured by the specified absorption rate (SAR); achieving maximum bandwidth, efficiency and minimum electrical size; reducing sensitivity to manufacturing tolerances. Material-coated antennas do appear to be less sensitive to detuning effects from obstacles in close proximity but how this relates to SAR is unknown. Measurements and computer simulation can provide design information on a specific antenna configuration but here we seek fundamental guidelines from the analysis of an exact canonical model based on separable spherical boundary conditions.

Analysis: A ceramic sphere of radius a (see inset in Fig. 1) is excited by either magnetic (TE) or electric (TM) multipole sources at the origin 0. The material relative permeability and permittivity are specified as:

$$\left.\begin{array}{ll}\mu_{r1} = \mu_1' + j\mu_1'', & \tan\delta_{\mu 1} = \mu_1''/\mu_1' \\ \varepsilon_{r1} = \varepsilon_1' + j\varepsilon_1'', & \tan\delta_{\varepsilon 1} = \varepsilon_1''/\varepsilon_1'\end{array}\right\} \quad r \le a$$
$$\varepsilon_{r2} = \varepsilon_2' + j\varepsilon_2'', \quad \tan\delta_{\varepsilon 2} = \varepsilon_2''/\varepsilon_2' \qquad r \ge a \tag{1}$$

thus allowing the antenna to operate in a lossy dielectric environment. The fields and sources have $\exp[-j\omega t]$ time dependence and are expressed in spherical eigenfunctions [5]:

$$\exp[jm\phi]P_n^m(\cos\theta)R(r), \quad n = 1, 2, 3, \ldots, \infty, \quad m = 1, 2, 3, \ldots, n$$

where (r, θ, φ) are spherical co-ordinates, $P_n^m(\cos\theta)$ are associated Legendre functions and $R(r)$ is either a spherical Bessel function $j_n(r)$ of the first kind or of the third kind $h_n^{(1)}(r)$. On invoking continuity of the tangential fields at $r = a$ for each (nm)th eigenfunction, the fields for $r \ge a$ have an amplitude governed by:

$$\frac{A_{nm}\{[\rho_1 h_n^{(1)}(\rho_1)]' j_n(\rho_1) - [\rho_1 j_n(\rho_1)]' h_n^{(1)}(\rho_1)\}}{K[\rho_2 h_n^{(1)}(\rho_2)]' j_n(\rho_1) - [\rho_1 j_n(\rho_1)]' h_n^{(1)}(\rho_2)} \tag{2}$$

where $[f(\rho)]'$ denotes differentiation of $f(\rho)$ with respect to ρ, A_{nm} is the (nm)th source amplitude, $\rho_1 = k_1 a$, $\rho_2 = k_2 a$, $k_1 = k_0(\mu_{r1}\varepsilon_{r1})^{1/2}$, $k_2 = k_0(\varepsilon_{r2})^{1/2}$, $k_0 = 2\pi/\lambda_0$, λ_0 = freespace wavelength and: